Accelerated apoptosis in the *Timp-3*–deficient mammary gland

See related Commentary on pages 799–800.

Jimmie E. Fata,[1] Kevin J. Leco,[1] Evelyn B. Voura,[1] Hoi-Ying E. Yu,[1] Paul Waterhouse,[2] Gillian Murphy,[3] Roger A. Moorehead,[1] and Rama Khokha[1]

[1]Ontario Cancer Institute/University Health Network, University of Toronto, Toronto, Ontario, Canada
[2]GlycoDesign, Toronto, Ontario, Canada
[3]School of Biological Sciences, University of East Anglia, Norwich, United Kingdom

Address correspondence to: Rama Khokha, Ontario Cancer Institute/University Health Network, University of Toronto, Toronto, Ontario M5G 2M9, Canada.
Phone: (416) 946-2051; Fax: (416) 946-2984; E-mail: rkhokha@oci.utoronto.ca.

Kevin J. Leco's present address is: Department of Physiology, University of Western Ontario, London, Ontario, Canada.

Roger A. Moorehead's present address is: Department of Biomedical Sciences, Ontario Veterinary College, University of Guelph, Canada.

Received for publication May 1, 2001, and accepted in revised form August 3, 2001.

The proapoptotic proteinase inhibitor TIMP-3 is the only molecule of this family thought to influence cell death. We examined epithelial apoptosis in TIMP-3–deficient mice during mammary gland involution. Lactation was not affected by the absence of TIMP-3, but glandular function, as measured by gland-to-body weight ratio and production of β-casein, was suppressed earlier during postlactational involution than in controls. Histological examination revealed accelerated lumen collapse, alveolar-epithelial loss, and adipose reconstitution in *Timp-3*$^{-/-}$ females. Epithelial apoptosis peaked on the first day of involution in *Timp-3*–null glands but at day 3 in wild-type littermates. Unscheduled activation of gelatinase-A was evident by zymography and correlated with earlier fragmentation of fibronectin in *Timp-3*$^{-/-}$ mammary. To obtain independent evidence of the proapoptotic effects of TIMP-3 deficiency, we introduced recombinant TIMP-3–releasing pellets into regressing *Timp-3*$^{-/-}$ mammary tissue and showed that this treatment rescued lumen collapse and epithelial apoptosis. Ex vivo, involuting *Timp-3*$^{-/-}$ mammary tissue demonstrated accelerated epithelial apoptosis that could be reduced by metalloproteinase inhibition. The physiological relevance of TIMP-3 became apparent as *Timp-3*$^{-/-}$ dams failed to reestablish lactation after brief cessation of suckling. Thus, TIMP-3 is a critical epithelial survival factor during mammary gland involution.

J. Clin. Invest. **108**:831–841 (2001). DOI:10.1172/JCI200113171.

Introduction

Pericellular proteolysis of cell surface molecules, extracellular factors, and ECM is intrinsically linked to cell function and fate (1, 2). Regulation of these multiple proteolytic processes is primarily achieved through coordinated interactions between proteinase, their biologic inhibitors, and the substrates. Tissue inhibitors of metalloproteinases (TIMP-1 to TIMP-4) are emerging as essential regulatory molecules, given their direct inhibitory function against two metzincin families of zinc-dependent proteinases involved in pericellular proteolysis; namely, the MMPs (matrix metalloproteinases) and the ADAMs (a disintegrin and metalloprotease) (3, 4). Although considerable literature supports the involvement of TIMPs in inhibiting cell migration, invasion, angiogenesis, and metastasis, the direct influence of TIMPs on cell fate remains little explored.

Although the four TIMP proteins share similar secondary and tertiary structures and in general are able to inhibit all MMPs albeit with varying degrees of affinity, TIMP-3 stands out as a unique member. For instance, unlike the other TIMPs, which after secretion become freely diffusible within the cellular microenvironment, TIMP-3 becomes tightly bound to the ECM (5–7). In addition, inherited mutations in *Timp-3* lead to Sorsby fundus dystrophy, a degenerative eye disease (8). Further, *Timp-3* silencing through promoter methylation is often found in cancer specimens (9, 10), whereas other TIMPs often show tumorigenic upregulation (3). TIMP-3 exhibits direct inhibitory activity against several ADAMs that are not inhibited by other TIMPs, including TNF-α convertase (TACE, ADAM-17) (11, 12), ADAM-12S (13), aggrecanase-1 (ADAM-TS4), and aggrecanase-2 (ADAM-TS5) (14). Likely through inhibition of ADAM-mediated ectodomain shedding, TIMP-3 also inhibits cell shedding of L-selectin (15) syndecans-1 and -4 (16), IL-6 receptor (17), c-MET (18), and cleavage of IGF binding proteins-3 and -5 (13). Finally, several reports have found that high levels of TIMP-3 are proapoptotic in both normal and cancer cell lines (19–24), and that the pro-death domain resides in its N-terminal domain (25). Using mammary gland involution as a model for physiological apoptosis and recently generated TIMP-3–deficient mice

(26), we explore here the physiological relationship between TIMP-3 and programmed cell death.

Few adult tissues exhibit extensive apoptosis under physiological conditions. These include the small intestine, adipose, uterus, ovary, and mammary gland (27–30). The latter, in response to diminishing lactational stimuli and milk buildup, undergoes postlactation involution that involves extensive epithelial apoptosis (31–33). Mammary gland involution is brought to completion by two proposed stages: the first deemed proteinase-independent, and the second, proteinase-dependent (34, 35). These stages bring about the depletion of milk-secreting lobulo-alveoli and the reversion of the gland to that resembling a prepregnant state. Experimentally, mammary involution is initiated and synchronized by removal of young suckling pups. In response to the cessation of suckling, stage one (a proteinase-independent stage) of mammary gland involution begins and lasts for approximately 3 days. Local mammary-derived signals such as milk accumulation and transcription of cell death genes that induce epithelial cell shedding and epithelial apoptosis are all characteristics of stage one. Stage two (the proteinase-dependent stage) occurs while lactogenic hormones begin decreasing and is primarily a stromal response involving further mammary epithelial apoptosis, phagocytosis by macrophages, lobulo-alveolar collapse, dissolution of the basement membranes surrounding the alveoli, and adipose reconstitution. Recolonization of the stroma by adipocytes, as they differentiate and accumulate lipids, has recently been considered a third stage of mammary gland involution and termed the biosynthetic stage (36).

During the second stage of mammary gland involution, cell-ECM survival signals are proposed to be lost through proteinase-mediated basement membrane degradation (35). This diminishing of survival signals, coupled with the gain of death signals during the first stage of involution, brings about irreversible loss of functional lactation (35). In other words, before proteinases are upregulated, dams are able to reinitiate lactation if suckling pups are returned. The increased activity of MMPs, serine proteinases, and cysteine proteinases is thought to mediate ECM degradation (34, 35, 37–40) and has recently been proposed, as in the case of stromelysin-1 (MMP-3), to determine the rate of adipose reconstitution (36). In coordination, several proteinase inhibitors also display tight regulation during mammary gland involution (34, 41–43). One function of these inhibitors may be to regulate and limit the amount of ECM degradation, as seen when high TIMP-1 levels are inappropriately maintained (41). Given that TIMPs, specifically TIMP-3, can inhibit many aspects of pericellular proteolysis, beyond just ECM degradation, a broader view of proteinase inhibitor function during mammary gland involution can be envisioned. However, it has yet to be determined whether or when any of these proteinase inhibitors are functionally essential during this tightly controlled process.

Here we show that initiation of epithelial apoptosis during mammary gland involution is inappropriately immediate in *Timp-3*–deficient mice. This is reflected in an early loss of milk production, cell shedding, a rapid loss of epithelial compartment, and epithelial cell apoptosis. Further, lack of TIMP-3 leads to an early unscheduled activation of gelatinase-A (MMP-2) and fibronectin fragmentation. These events were reversed upon biochemical reconstitution with recombinant TIMP-3 or a synthetic metalloproteinase inhibitor (MPi). Importantly, compared with the wild-type dams, *Timp-3*$^{-/-}$ dams could not reestablish lactation when suckling was prevented for 2 days during involution. These findings demonstrate that TIMP-3 is not expendable during mammary gland involution. It functions during the first stage of this process, in part, by inhibiting the onset of second stage, proteinase-dependent ECM degradation, and regulates the kinetics of cell death and tissue turnover. To our knowledge, this study also provides the first genetic evidence that TIMP-3 deficiency enhances physiological apoptosis.

Methods

Experimental animals. Mice genetically deficient for *Timp-3* were generated as described (26) and were backcrossed six times into an FVB background for the studies described here. The *Timp-3*–null mice were viable in the absence of TIMP-3 protein. All experiments were performed on 6- to 8-week-old primiparous *Timp-3*–null and wild-type female littermates. At this age, *Timp*-3–null dams did not display signs of abnormal lung function, which only becomes evident after 1 year of age (26). No differences in litter size or pup weight gain during nursing was evident between *Timp-3*, *Timp-3* heterozygous, and wild-type mice. As well, nursing characteristics of *Timp-3*–null dams were not different than those of wild-type dams. All animals were cared for and sacrificed in accordance with guidelines of the Canadian Council for Animal Care.

Induction of synchronized involution and collection of mammary tissue. In both experimental (*Timp-3*$^{-/-}$) and control groups (wild-type), litter size was kept at six pups to maintain even suckling frequency on each teat and minimize intermouse mammary gland variation. To synchronize involution, litters were removed from dams after 10L. Twenty-four hours later was considered day 1 of involution (1di), with all subsequent days being designated appropriately. Mammary glands (second/third thoracic and the fourth/fifth inguinal) were collected at various time points of involution and either fixed in 4% buffered formalin for 24 hours or frozen on dry ice. Before this, one entire fourth inguinal was weighed and divided by the whole-body weight of the mouse to calculate the mammary to body weight index.

Histology, electron microscopy, and histomorphometry. Histological analysis was performed on hematoxylin and eosin–stained 5-μm sections. To compare the kinetics of involuting tissue between *Timp-3*–null and wild-type mammary glands, we analyzed several histological criteria at 43× magnification using a Mertz graticule. The fields examined (six in total) were adjacent to each other, the first field being immediately distal to the lymph node of the fourth inguinal mammary gland, and all

subsequent fields moving away from this structure. On several samples, histomorphometry was performed on many successive sections from the same mammary tissue to determine whether intramammary variation affected these areas. Two criteria were selected for histomorphometry. These included the presence or absence of a lumen or an adipocyte. The percentage contribution of each criterion was then calculated for each field and averaged over six fields. For electron microscopy, mammary tissue squares (1 mm^3) isolated from the area immediately distal to the lymph node were fixed in 4% buffered formalin overnight, washed extensively in PBS, and stored in 70% EtOH before viewing.

Hoechst staining for apoptotic cells. To visualize cellular apoptosis in mammary tissue undergoing involution, 5-μm sections from the fourth inguinal, were dewaxed for 2 separate 5 minute sessions in toluene, hydrated by 5 minutes in 100%–90%–70% EtOH and H_2O and stained in Hoechst dye for 30 minutes. Sections were then dehydrated through EtOH and dipped in toluene for cover slipping. Under ultraviolet light microscopy, those cells exhibiting nuclear condensation and fragmentation were determined apoptotic. Cell death indices (apoptotic nuclei/total nuclei × 100%) were generated based on counting of no less than 500 nuclei in ten fields immediately distal to the lymph node.

Statistical analysis. Histomorphometry and apoptosis indices (average ± SEM) were performed on a total of 28 mice, with at least two mice from each time point per group. Statistical comparisons at each time point involved using a one-tailed Student's *t* test.

Protein isolation. From each animal, the second and third thoracic mammary glands were homogenized in 500 μl of either extraction buffer (1% Triton X-100, 500 mM Tris-HCl [pH 7.6], 200 mM NaCl, and 10 mM $CaCl_2$) for zymography or lysis buffer (10 mM Tris [pH 7.6], 5 mM EDTA, 50 mM NaCl, 1% Triton-X, 30 mM tetra-sodium pyrophosphate, 200 μM sodium orthovanadate, 1 mM PMSF, 5 μg/ml aprotinin, 1 μg/pepstatin, 2 μg/ml leupeptin) for immunoblotting. The homogenates were centrifuged at 12,000 *g* for 20 minutes at 4°C and the supernatant and insoluble pellets were stored at –70°C until needed. Protein concentration was determined using Bradford assay reagents (Bio-Rad Laboratories Inc., Hercules, California, USA).

Zymography. Mammary lysate (40 μg/lane) was added to 4X sample buffer (10% SDS, 4% sucrose, 0.25 M Tris [pH 6.8]) and resolved on a 10% polyacrylamide gel (SDS-PAGE) containing 0.1% gelatin. After electrophoresis, the gels were rinsed in 2.5% Triton X-100, two times for 30 minutes, followed by incubation for 24 hours at 37°C in substrate buffer (50 mM Tris [pH 7.5], 5 mM $CaCl_2$, 40 mM NaN_3). Gels were stained in Coomassie brilliant blue for 30 minutes at room temperature, followed by destaining (50% methanol, 10% acetic acid).

Western blotting. Mammary lysate (40 μg/lane) was resolved in a 6% polyacrylamide gel under reducing conditions. Proteins were transferred to Hybond ECL nitrocellulose membranes (Amersham Pharmacia Biotech, Buckinghamshire, United Kingdom), and membranes were blocked in 5% skim milk in Tris-buffered saline containing 1% Tween (TBST) for 2 hours at room temperature. Fibronectin antibody (H-300; Santa Cruz Biotechnology Inc., Santa Cruz, California, USA) was incubated at 1:500 in 5% skim milk in Tris-buffered saline with 0.1% Tween overnight at 4°C. Similarly β-casein mAb was incubated at a dilution of 1:1,000 in 5% BSA. Detection was performed using an anti-rabbit secondary antibody and LumiGlO reagents (New England Biolabs Inc., Beverly, Massachusetts, USA).

Ex vivo mammary gland culture. Mice were sacrificed on day 10 of lactation. All mammary glands were excised into DMEM media and chopped into 1-mm^3 pieces. A total of 60 mg of the pieces was placed into a 30-mm dish containing 3 ml DMEM supplemented with 10% FBS and 5 μg/ml each of hydrocortisone, insulin, and prolactin. This medium has been shown to maintain mammary cells and tissue in a relative healthy state; however, apoptotic turnover of the tissue does occur. The synthetic metalloproteinase inhibitor Ilomastat (10 μM; AMS Scientific, Concord, California, USA) was included when indicated. At the indicated time, cultures were washed three times in HBSS and tissues were snap frozen for processing or fixed in 10% formalin for sectioning. Formalin fixed sections were examined for apoptotic nuclei with Hoechst stain, as described above, and counterstained in 0.0025% eosin for 15 seconds. Multiple 1 μm sections were then visualized for apoptotic cells using a Zeiss Axiovert S100 microscope equipped with 510 confocal software (Carl Zeiss Ltd., Toronto, Canada).

Recombinant TIMP-3 slow release pellets. Ethylene vinyl acetate (Elvax-40) pellets (a gift from Dupont, Boston, Massachusetts, USA) containing recombinant TIMP-3, were generated and implanted as described previously (44, 45). All recombinant TIMP-3 (5 μg/pellet) and control pellets were surgically implanted into the fourth mammary fat pad distal to the lymph node. Each mouse received one pellet containing recombinant TIMP-3 and one control pellet into the contralateral mammary gland 1 day before removing pups (10L). Mammary glands that contained a pellet were collected 2 days after removing pups (2di).

Reinitiation of lactation. Pup weight gain or loss was analyzed in 10-day-old wild-type litters ($n = 6$) placed with dams (*Timp-3*–null and wild-type mice) that had had their pups removed 2 or 3 days before. Pup weight was measured upon the initial placing ($t = 0$) and every 24 hours later for 7 days. An average litter weight was calculated, and the gain or loss from original litter weight ($t = 0$) was determined. Experiments were terminated if pups lost more than 15% of their original weight, at which time they were rescued with surrogate lactating dams.

Results

Earlier loss of glandular function in Timp-3–null mice. The mammary gland weight to body weight ratio reflects milk accumulation during pregnancy and loss during involution. At day 10 of lactation, this ratio was similar between the wild-type and *Timp-3*–deficient dams (Figure

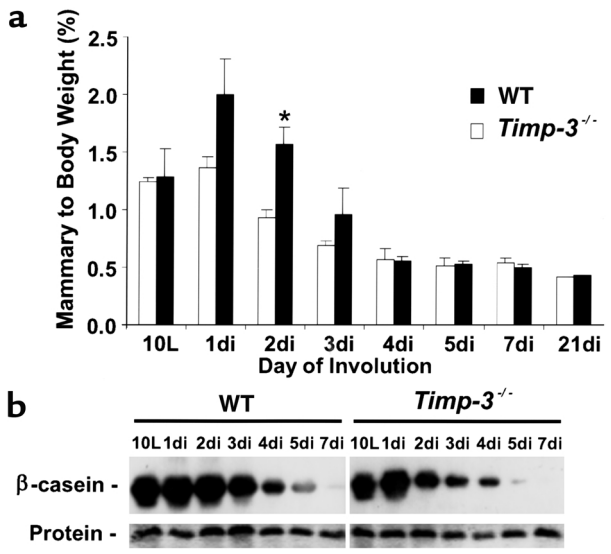

Figure 1

Early loss of milk secretion and β-casein expression in *Timp-3*–null mammary glands during involution. (**a**) Upon initiation of involution, the mammary gland to body weight ratio increased in wild-type (WT) mice but not in *Timp-3*–null mice. Significant differences were found at 2di. **P* < 0.05. No differences were found thereafter. All time points were derived from at least *n* = 2 mice per genotype and are shown as mean ± SEM. (**b**) β-Casein protein declined rapidly after 1di in *Timp-3*–null mice compared with its gradual loss in wild-type mice. Immunoblot is representative of two separate experiments. Equal loading was confirmed by staining the membrane with Amido Black.

1a), indicating comparable lactation ability in these mice. Upon initiation of involution, milk initially builds up in the mammary gland and is typically reflected as increased mammary to body weight ratio. This was observed in wild-type female mice at 1di and 2di. (Figure 1a). In contrast, no rise in this ratio was apparent in *Timp-3*–null female mice, with significant differences being reached at 2di (Figure 1a; $P < 0.05$). With the loss of milk synthesis that invariably occurs during involution (4di and onward), the mammary gland to body weight ratios in both genotypes decreased to the baseline, nonpregnant state (Figure 1a). Next, we compared β-casein expression, the major milk protein, between wild-type and *Timp-3*–null mammary glands. In wild-type mice β-casein mRNA (data not shown) and protein levels (Figure 1b) declined as involution proceeded, with a noticeable lowering at 4di. This differed from *Timp-3*–deficient mice, in which the reduction in β-casein protein was apparent as early as 2di (Figure 1b). These observations provided the first indication that *Timp-3*–deficient mice incur an immediate repression of epithelial glandular function upon initiation of involution.

TIMP-3 maintains lumen structure and delays adipose reconstitution. During lactation, secretory epithelial cells constitute the glandular structure in mammary tissue. After 10L, we observed no histological differences between the epithelial glandular network in mammary glands from wild-type and *Timp-3*–null mice (data not shown). However, in mammary glands undergoing involution, gross histological differences were revealed between *Timp-3*–deficient and wild-type mice (Figure 2, a–p). Specifically, *Timp-3*–deficient mammary glands at 1di exhibited substantial cell shedding into the lumen (Figure 2, a, e, i, and m). Alveolar and lumen collapse was obvious along with adipose reconstitution at 2di (Figure 2, b, f, j, and n), and epithelial chords were visible by 3di in *Timp-3*–deficient tissue (Figure 2, g and o). In stark contrast, the wild-type glands at days 1 and 2 of involution still resembled those of 10L, with a considerable number of apparently functional lumens. Therefore, the morphological kinetics of mammary gland involution were altered in mammary glands from *Timp-3*–deficient mice. To quantify these differences between each genotype, histomorphometric analysis was used to determine the percentage of the mammary gland occupied by lumens or adipose. In *Timp-3*–null mammary glands, a precipitous decline in lumens was apparent between 2di and 3di, whereas the peak of adipose reconstitution was seen at 4di (~70% of tissue was adipose). Mammary glands from wild-type mice, however, showed the majority of luminal loss between 3di and 4di, and maximal adipose reconstitution was not achieved until 7di (Figure 2q). Overall, these data indicate that mammary involution was markedly accelerated in *Timp-3*–null female mice. Using transmission electron microscopy to visualize differences at the ultrastructural level, we found that 10L mammary glands were comparable between both genotypes (Figure 2, r and s). At 1di, granular secretions, most likely of proteinaceous origin, became apparent on the basal side within the interstitial matrix in *Timp-3*–deficient mammary tissue (Figure 2u). Such substance was only found secreted in a polar fashion into the luminal side in wild-type tissue at 1di (Figure 2t). Extensive fillopodia were often evident on the basal side of mammary epithelium from *Timp*-3–null mice, which produced a more convoluted, although intact, basal lamina when compared with wild-type basal lamina (Figure 2, s and u; data not shown). These electron microscopy observations suggest an immediate disassembly of cell-cell contact in glandular structures and/or an early loss of secretory cell polarity in *Timp-3*–deficient mammary tissue.

Attainment of maximal apoptosis at 1di in Timp-3–null mice. Postlactational involution of the mammary gland is dependent on extensive epithelial apoptosis (31–35). Epithelial cells with nuclear condensation were abundant in the lumens at 1di in *Timp-3*–deficient mammary tissue, whereas such cells did not predominate until 3di in wild-type tissue (Figure 3, a–d). Apoptotic cells were primarily found in lumena during the first 3 days of involution for wild-types and for the first 2 days of involution in *Timp-3*–null tissue. After these time points, when lumena collapse, apoptotic cells were located within epithelial chords. Derivation of an epithelial apoptotic index revealed a characteristic profile with a peak at 3di (Figure 3e) in wild-type mice. Remarkably, the peak of epithelial apoptosis occurred at 1di in *Timp-3*–deficient mammary tissue (Figure 3e). Significant differences in apoptotic indices existed between the two geno-

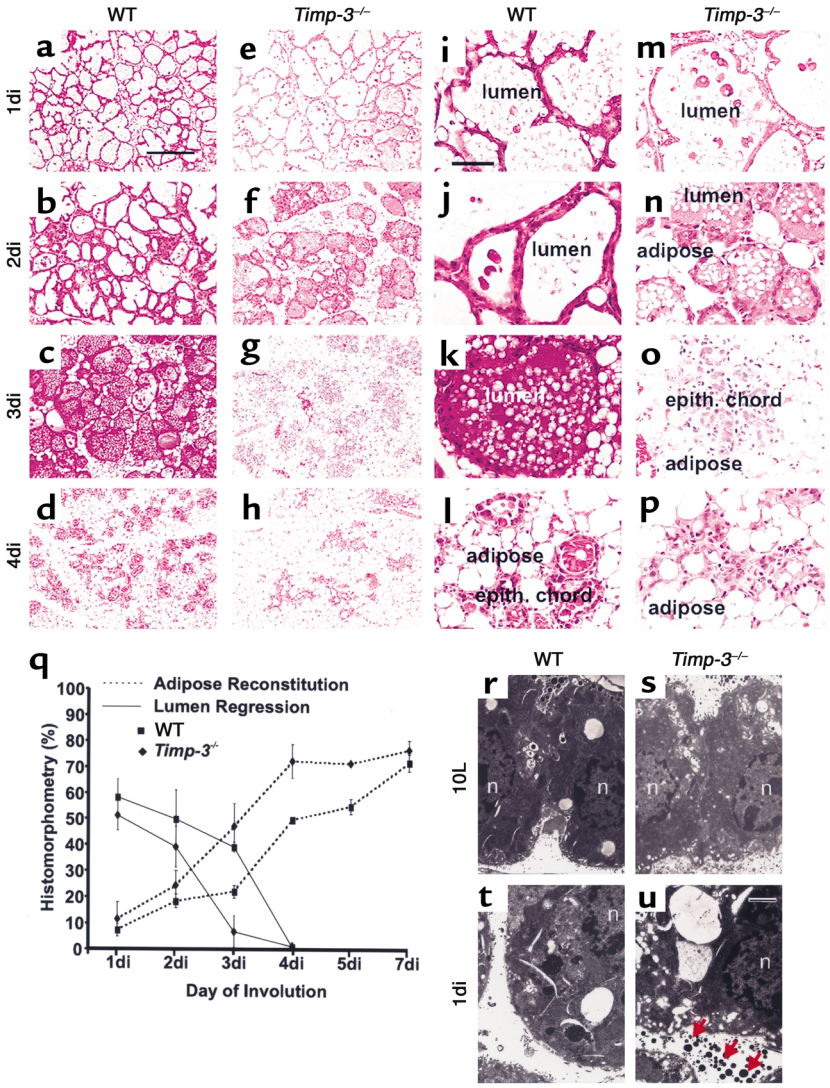

Figure 2
TIMP-3 regulates kinetics of mammary gland involution. (**a**–**p**) H&E–stained involuting mammary glands from wild-type (**a**–**d** and **i**–**l**) and *Timp-3*–null (**e**–**h** and **m**–**p**) female mice. At 1di, more cell shedding into the lumen was evident in *Timp-3*–deficient mammary glands (**e** and **m**) compared with controls (**a** and **i**). Lumen regression and adipose reconstitution occurred at 3di in mammary glands from wild-type mice (**c** and **k**). In contrast, lumen regression and adipose reconstitution occurred as early as 2di in mammary glands from *Timp-3*–null mice (**f** and **n**). Epithelial chords (epith. chord) were evident 1 day earlier (3di) in *Timp-3*–deficient mammary glands compared with wild-type mammary glands (compare **g** and **o** with **d** and **l**). (**q**) Histomorphometric analysis revealed lumen regression (solid line) was rapid between 2di and 3di in *Timp-3*–null mammary glands, whereas regression of lumens occurred between 3di and 4di in wild-type mammary glands. Adipose reconstitution (dotted line) was approximately 70% of the tissue by 4di in *Timp-3*–null mammary glands. This value was not reached until 7di in wild-type mammary glands. (**r**–**u**) At 10 days of lactation (10L) electron microscopy of secretory epithelial cells revealed that apical secretions into the lumen occurred in both wild-type and *Timp-3*–null mammary glands. However, at 1di these secretions (red arrows) were evident on the basal side of *Timp-3*–null epithelial cells within the interstitial matrix, whereas they were still only found apically in wild-type tissue. Scale bars in **a**–**h**, 100 μm, and in **i**–**p**, 50 μm; ×9,000 in **r**–**u**.

types at 1di and 3di ($P < 0.05$). From 4di onward, however, the apoptotic indices were comparable in these groups. Importantly, the total amount of epithelial loss was equivalent in *Timp-3*–deficient involuting mammary glands compared with wild-types. These data demonstrate that the absence of TIMP-3 in mammary tissue during involution accelerates the kinetics of epithelial apoptosis, while not increasing the overall cell death.

Unscheduled activation of MMP-2 in Timp-3–deficient involuting mammary tissue. Activation of latent MMP-2 (68 kDa) to activated MMP-2 (60 kDa) is known to occur in mammary gland at 3di (41, 42). This matrix proteinase is thought to mediate the removal of basement membrane components surrounding alveoli and promote tissue remodeling. Zymography was performed to determine the MMP activity in the wild-type and *Timp-3*–deficient tissues. As was expected, we found MMP-2 activation at 3di, which lasted until 7di in wild-type regressing mammary glands (Figure 4a; data not shown). In contrast, a low level of activated MMP-2 was found as early as 1di in *Timp-3*–deficient mammary tissue (Figure 4b). Similar levels of the latent form of MMP-9 (~105 kDa) were seen in both wild-type and *Timp-3*–null mammary glands. Early activation of MMP-2 in *Timp-3*–null mammary glands undergoing involution provides one explanation of why these tissue regress faster than wild-type mammary glands.

Early fibronectin fragmentation in Timp-3–null involuting mammary tissue. The glycoprotein fibronectin is found in both basement membrane and interstitial stromal matrix in the mammary gland (46). An upregulation of fibronectin protein at 4–6di and fibronectin fragmentation around 4di have previously been reported (47). A similar change in fibronectin profile, and fragmentation was seen at 3di in our wild-type mice (Figure 5). In *Timp-3*–null mammary glands, fibronectin levels did not display an increase around 4–6di. Further, fibronectin fragmentation was apparent earlier at 2di (Figure 5), which was reproducible in an independent experiment. Our analysis of laminin in mammary gland involution showed no fragmentation of this protein in either wild-type or *Timp-3*–deficient tissues (data not shown). Deficiency of TIMP-3 therefore promoted earlier fragmentation of fibronectin, but not of laminin, during mammary gland involution.

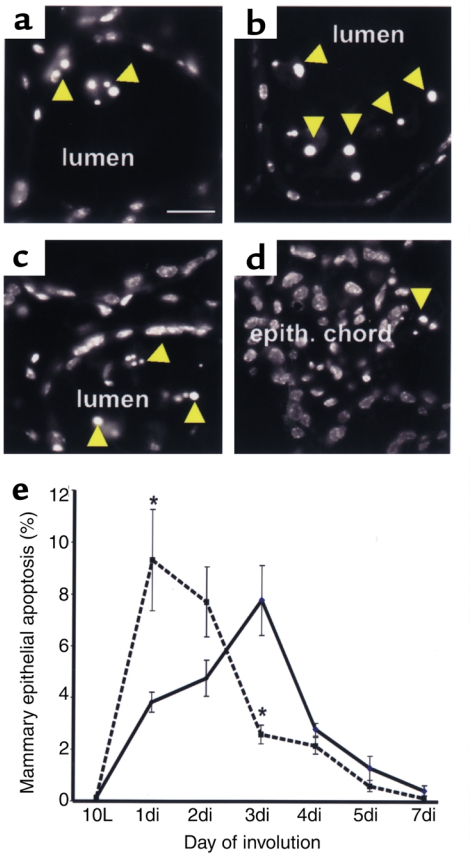

Figure 3
(**a** and **b**) Hoescht stain revealed numerous apoptotic bodies (yellow arrow) within lumens of *Timp-3*–null mammary glands at 1di, compared with markedly less in wild-type lumens at 1di. (**c** and **d**) Many apoptotic bodies were evident at 3di within still-existing lumens of wild-type tissue. In contrast, at 3di, few lumens existed in *Timp-3*–deficient tissue, and apoptotic cells were less abundant. (**e**) Quantification of apoptosis in involuting mammary glands from both genotypes revealed clear differences in the rate of cell death. The amount of apoptosis in wild-type tissue during mammary gland involution peaked at 3di. In contrast, apoptosis peaked at 1di in *Timp-3*–null mammary gland, with successive decreases thereafter. Significant differences in the amount of apoptosis between involuting wild-type and *Timp-3*–deficient mammary glands were found at 1di and 3di. $*P < 0.05$. The total amount of apoptosis from 10L to 7di did not significantly differ between wild-type and *Timp-3*–deficient mammary glands. Images and quantifications are derived from the area immediately distal to the lymph node. Scale bar in **a**–**d**, 50 μm.

Rescue of the proapoptotic phenotype in vivo by recombinant TIMP-3. Given that TIMP-3 overexpression has been shown to promote cell death (19–24), our phenotype of enhanced epithelial apoptosis in the absence of TIMP-3 was unexpected. Therefore, independent approaches were used to substantiate our findings on apoptosis. We determined whether increased epithelial apoptosis in *Timp-3*–deficient mammary tissue could be rescued by biochemical reconstitution with TIMP-3 protein. Elvax slow-release pellets (Dupont, Boston, Massachusetts, USA) containing human recombinant TIMP-3 (rTIMP-3) protein were implanted into *Timp-3*$^{-/-}$ mammary glands at 10L, pups were then immediately removed, and mammary glands were examined days later (2di). Mammary tissue with rTIMP-3 pellet showed a local maintenance of luminal alveoli when compared with the control pellet-bearing contralateral tissue (Figure 6, a and b). Further, apoptosis was significantly retarded near implanted rTIMP-3 pellets (Figure 6, a–c). Thus, reconstitution of TIMP-3–depleted mammary tissue for 2 days with rTIMP-3 resulted in a rescue of early lumen collapse and impeded induction of unscheduled apoptosis.

Enhanced apoptosis in cultured Timp-3–deficient mammary tissue can be inhibited by a synthetic metalloproteinase inhibitor. Next, we turned to an ex vivo approach, to determine whether we could biochemically manipulate mammary epithelial apoptosis with a synthetic metalloproteinase inhibitor (MPi; ilomostat) that exhibits both MMP and ADAM inhibition. Representative eosin- and Hoescht-stained sections of ex vivo cultures established from day 10 of lactation (day 0) and maintained over a 6-day period in presence or absence of MPi are shown in Figure 7, a–f. The wild-type and *Timp-3*–null cultures were comparable at day 0. Typically during culture, milk was lost from the alveolar structures, which permitted compaction of alveoli. "Ghostlike" structures remained, owing to lack of cell clearance and adipocyte reconstitution, which normally occur in vivo. At the morphological level, there was a slow decline in cell number in the wild-type tissue over the 6-day period (Figure 7, a and b), whereas *Timp-3*–null tissue showed a remarkable loss in cellularity (Figure 7, d and e). Notably, this loss of cellularity was substantially reduced in *Timp-3*–null cultures maintained in the presence of MPi for 6 days and was similar to that of untreated wild-type mammary tissue at day 6 (Figure 7, e–g). We measured epithelial apoptosis in these sections at days 4–6 of culture. Significantly, greater apoptosis was observed in *Timp-3*–deficient mammary glands compared with the control wild-type tissue (Figure 7h; $P < 0.01$ and data not shown). Addition of 10 μM MPi modestly reduced the elevated apoptosis in *Timp-3*–deficient tissue (Figure 7h;

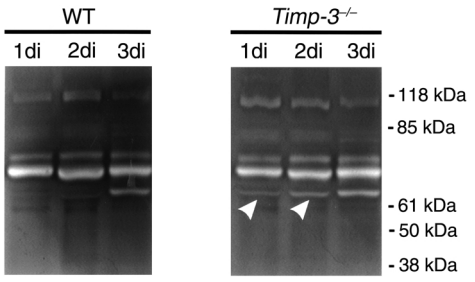

Figure 4
Gelatin zymography of mammary protein extracts from 10L to 3di from wild-type and *Timp-3*–null mammary glands. Activation of pro–MMP-2 (70-kDa and 68-kDa bands) to an active form (62 kDa) occurred at 3di in wild-type mammary tissue. In contrast, the activated species was evident during lactation and at 1di and 2di of involution in *Timp-3*–deficient mammary glands (arrowheads). The upper band (~105 kDa) in both zymograms likely represents pro–MMP-9 and did not show differential regulation.

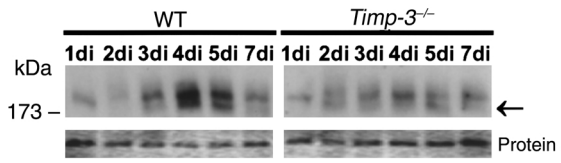

Figure 5
Fibronectin fragmentation occurred earlier in *Timp-3*–null mammary gland involuting. Under denaturing and reducing conditions intact fibronectin migrates to 220 kDa and is present at all time points of involution in both *Timp-3*–null and wild-type tissue. Fragmentation of this mature form occurred 1 day earlier in *Timp-3*–null mammary glands than in wild-type (arrow). Equal loading was confirmed by staining the membrane with Amido Black.

$P < 0.07$), although epithelial apoptosis still remained higher than the wild-type controls. This indicated that the *Timp-3*–deficient tissue retains its increased susceptibility to apoptosis in this ex vivo assay. The epithelial apoptosis is impeded, although not completely attenuated, through inhibition of metalloproteinase activity.

Timp-3–null mice fail to reestablish lactation efficiently. The primary biologic function of the mammary gland is to provide nourishment to suckling young in the form of milk. Murine mammary glands forced to undergo involution have the ability to maintain function if the pups are placed back after approximately 48 hours, but lose this ability after approximately 60 hours (35). These findings were also seen in our studies, as wild-type dams at 3di failed to adequately nourish pups (measured by pup weight), whereas 2di dams could (Figure 8; data not shown). When we examined the ability of *Timp-3*–null dams at 2di and 3di to reinitiate lactation, we found that neither could nourish pups properly (Figure 8; data not shown). Moreover, these results did not depend on the genotype of the pups, indicating the defect is a function of the *Timp-3*–null mouse. Importantly, *Timp-3*–null dams with pups added back exhibited nursing characteristics not unlike those of wild-type dams in the same situation, suggesting the defect is not psychological. Pups placed back with *Timp-3*–null dams after 2di failed to gain weight for up to 7 days (Figure 8). In contrast, pups placed back with wild-type dams began gaining weight after 3 days of suckling (Figure 8). The inability of *Timp-3*–null mice to reestablish lactation after 2 days of involution demonstrates that TIMP-3 is an integral component of maintaining mammary gland function during the early stages of involution.

Discussion

The kinetics of murine mammary involution with respect to epithelial apoptosis, reduction in milk production, and tissue remodeling have been extensively studied by many investigators (31–35). The process is conserved across mammalian species and is a necessary event for returning the mammary gland to that resembling nulliparous tissue. In the present study, we demonstrate that TIMP-3 is an essential regulator of mammary gland involution. The *Timp-3*–deficient mammary gland exhibited extensive epithelial cell shedding and apoptosis on the 1st day of involution, as opposed to these events normally occurring on 3di and 4di. This unscheduled epithelial cell death led to an early loss of β-casein expression, rapid lobulo-alveolar collapse and early adipose differentiation and reconstitution. At the ultrastructural level, cell-cell adhesion was possibly breached, as basally located proteinaceous secretions were evident within 1di. Further, early activation of the basement membrane degrading metalloproteinase, MMP-2, and unscheduled fragmentation of fibronectin were apparent in *Timp-3*–deficient involuting mammary glands. Restoring TIMP-3 activity through implanted slow release pellets confirmed that this MMP inhibitor is antiapoptotic during mammary gland involution. Moreover, we show that an upregulation of metalloproteinase inhibition through a synthetic inhibitor was also antiapoptotic in an ex vivo model of mammary gland involution. Finally, the physiological significance of mammary TIMP-3 was highlighted, as the Timp-3–deficient female mice failed to reestablish lactation after the onset of involution. To our knowledge, this study is the first to demonstrate that an inhibitor of an extracellular proteinase is necessary for maintaining the conserved processes of mammary gland involution and function. Moreover, deficiencies in TIMP-3 function led to excessive and unscheduled physiological apoptosis in mammary epithelium.

Mammary gland involution and the TIMP/MMP axis. Three distinct stages have now been ascribed to the regressing mammary gland (34–36). The first stage is considered proteinase-independent. It entails milk accumulation, induction of genes involved in mediating apoptosis, the beginning of epithelial cell shedding, and epithelial apoptosis. The second, proteinase-dependent stage begins around 4di and is characterized by a decrease in lactogenic hor-

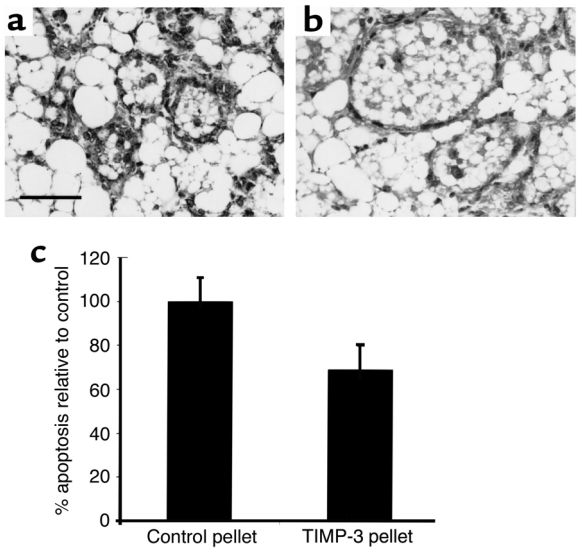

Figure 6
Exogenous addition of recombinant TIMP-3 through slow-release pellets maintained alveolar structure in involuting *Timp-3*$^{-/-}$ mammary glands (**a** and **b**). Quantification of apoptotic cells showed a marked decrease in involuting mammary gland treated with recombinant TIMP-3 when compared with contralateral mammary gland implanted with a control pellet (**c**). Scale bar, 50 μm.

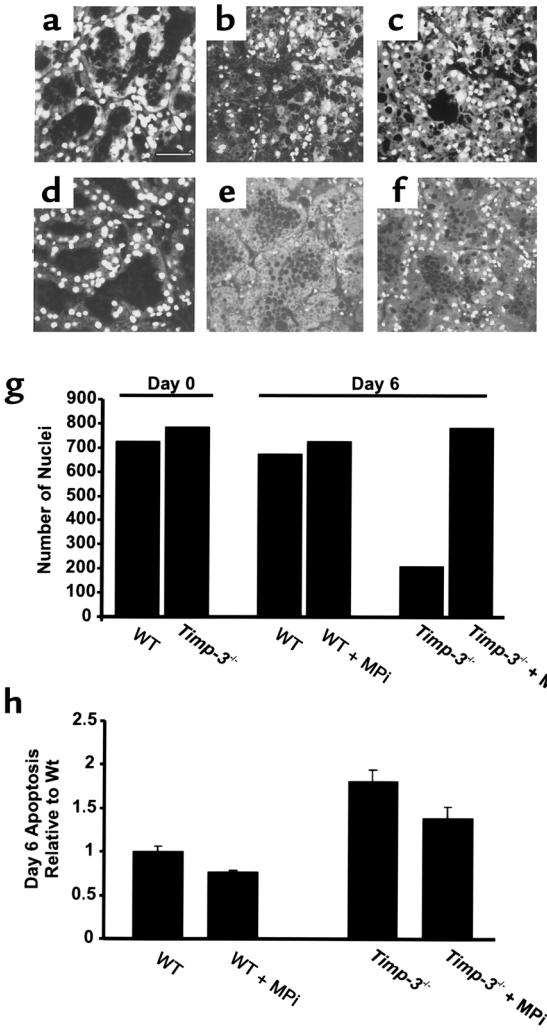

Figure 7
Inhibition of ex vivo mammary gland involution by a metalloproteinase inhibitor. Mammary gland cultured in an ex vivo assay displayed glandular structure that was indistinguishable between wild-type and *Timp-3*–null genotypes at day 0 (compare **a** with **d** and **g**). After 6 days in culture, gross differences were found between each genotype reflected as increased loss of nuclei (compare **b** with **e** and **g**), and greater apoptosis (**h**) in *Timp-3*–deficient tissue. After 6 days in culture, the addition of a metalloproteinase inhibitor (Ilomastat, 10 μm) rescued nuclear loss (**f** and **g**) and inhibited apoptosis (**h**) in *Timp-3*–deficient mammary tissue. The metalloproteinase inhibitor did not overtly affect the glandular architecture of wild-type mammary glands (**c**) but did decrease the amount of apoptosis in this tissue (**h**). Scale bar, 50 μm.

mones, collapse of glandular structure, epithelial apoptosis, and basement membrane dissolution. The last stage, recently termed the biosynthetic stage, is rate-determined by proteinase activity and involves adipose differentiation and reconstitution. Because characteristics of first stage, second stage, and third stage inappropriately occurred in *Timp-3*–null female mice, we suggest that this inhibitor, at least in part, temporally regulates all three stages.

Matrix degrading proteinases clearly have an important function as mediators of the tissue remodeling that occur during mammary gland involution. The expression of these proteinases (MMP-2, MMP-3, and MMP-11) is tightly regulated (34, 36, 40, 42, 43), and their activity coincides with basement membrane degradation and tissue remodeling. TIMP mRNA levels during mammary gland involution have been shown to be both regulated, as in the case of TIMP-1 (41), and constitutive, as shown with TIMP-2 (34). In the *Timp* family, it appears that only TIMP-1 shows differential regulation, as we have found both TIMP-3 and TIMP-4 to be also constitutive, similar to that seen with TIMP-2 (data not shown). Importantly, the mammary glands of *Timp-3*–null tissue did not display any compensation by other Timps (data not shown), as we have reported for lung, heart, and kidney (26). Talhouk et al., in 1992, provided the first evidence of TIMP function in regulating this proteolytic activity, as TIMP-1 slow-release pellets maintained glandular architecture during mammary gland involution (41). In the present study, we show that rTIMP-3 also maintains glandular architecture and, furthermore, that it impedes cell death. These results would suggest that both TIMPs are antiapoptotic during mammary gland involution. Intriguingly, however, transgenic overexpression of TIMP-1 during mammary gland involution does not inhibit epithelial cell death, but instead enhances adipose reconstitution (36). In the same study, MMP-3–deficient mice exhibit enhanced mammary gland adipogenesis during involution. This led the authors to conclude that MMPs, at least those inhibited by TIMP-1, function as determinants of the rate of adipogenesis during mammary gland involution, and not as inducers of the epithelial cell death. We extend this hypothesis by indicating that proteinases efficiently inhibited by TIMP-3, but not TIMP-1, mediate cell death during mammary gland involution. Furthermore, depletion of the parenchymal compartment invariably induces a stromal response leading to adipose reconstitution. This is likely contributing to early adipogenesis in *Timp-3*–deficient mammary tissue.

Based on our finding of early MMP-2 activation in *Timp-3*–deficient involuting mammary glands, we propose that MMP-2 proteolytic activity is important in mediating the mammary epithelial cell death during involution. TIMP-2, considered a strong inhibitor of MMP-2, is expressed constitutively during mammary gland involution (34). MMP-2 mRNA has been localized to both myoepithelial cells and stromal fibroblasts within the mouse mammary gland (34, 47), and we have reported that TIMP-3 mRNA is expressed in the mouse mammary gland and localizes to mammary epithelium and myoepithelium (44, 48). This intimate spatial relationship between MMP-2 and TIMP-3 may provide one level of MMP-2 regulation. It also remains possible that other MMP activities, such as stromelysins or collagenase 3, are similarly enhanced in *Timp-3*–deficient regressing mammary tissue. Earlier activation of MMP-2 may have occurred through several possible mechanisms. First, as TIMP-3 is capable of inhibiting MT1-MMP (49), a known activator of pro–MMP-2 (50), absence of this inhibition may lead to an increase in MMP-2 activation. Another way

in which TIMP-3 can influence MMP-2 activation is through its close sequestration on proteoglycans. Both TIMP-3 and MMP-2 contain domains that mediate their sequestering by negatively charged proteoglycans (6, 7). In our model, pro–MMP-2 is free of TIMP-3–mediated ECM sequestration; therefore, it may be more readily activated. Finally, our finding of increased fibronectin fragmentation in *Timp-3*–deficient mammary glands may also promote MMP-2 activation, as fibronectin fragments have been shown to upregulate MMP activity (47, 51), including MMP-2 (52). In our other studies on the *Timp*-3–deficient mouse, we have observed spontaneous development of air space enlargement in the lung, have observed collagen loss, and have visualized heightened gelatinase activity in lung sections by in situ zymography (26). Together, our findings demonstrate that increased gelatinase activity may be a common mechanism by which loss of TIMP-3 affects tissue integrity and homeostasis.

Mechanisms that may underlie unscheduled mammary epithelial apoptosis in Timp-3–deficient tissue. How TIMP-3 modulates epithelial apoptosis during mammary gland involution may be attributed to two of its known functions. These are the ability to maintain ECM-mediated cell survival signals and the ability to inhibit shedding of cell surface molecules involved in apoptotic signaling. We provided evidence that unscheduled ECM degradation during mammary gland involution occurred in the absence of TIMP-3. In this study, the upregulation of MMP-2 activity shifts the balance toward matrix degradation around 3di and is concomitant with the peak of epithelial cell death in wild-type mice (41, 42). This shift occurred immediately in the absence of TIMP-3, and it may have led to an earlier depletion of ECM survival signals, which induced apoptosis. We further provide direct evidence that TIMP-3 maintains ECM stability in the mammary gland, as its deficiency led to early fibronectin fragmentation. Fibronectin has been localized to the interstitial matrix surrounding mammary epithelium and within mammary epithelial basement membrane (46, 53). Importantly, fibronectin can maintain cell survival (47, 54, 55), whereas fibronectin fragments promote cell apoptosis (47, 56). It has been reported that extensive fibronectin fragmentation corresponds to the peak of epithelial apoptosis during mammary gland involution (57). We observed unscheduled fibronectin fragmentation in *Timp-3*–deficient mammary glands undergoing involution. Although this early shift in fibronectin fragmentation may be conducive to epithelial cell death, it remains to be established whether fibronectin fragmentation is causal or consequential to the rapid mammary gland involution found in TIMP-3–deficient mice.

TIMP-3 may also influence mammary epithelial apoptosis during involution through its ability to inhibit ectodomain shedding of apoptotic regulating factors. For instance, an upregulation of TIMP-3 stabilizes TNF-α receptors on cell membranes and promotes cell death in colon carcinoma cells (23). TIMP-3 also exhibits inhibitory activity against TACE (11), which processes cell-bound TNF-α to its soluble, proapoptotic form (58). It may be that this latter factor is more prevalent in the absence of TIMP-3, a circumstance in which TACE activity may go unchecked. During lactation and involution, mammary epithelial cells are known to express TNFR (59), and, importantly, soluble TNF-α has been found in the lumens of bovine involuting mammary glands (60). Fas-L, another member of the TNF-α superfamily, may also be more abundant in *Timp*-3–null tissue. This factor becomes proapoptotic in mouse involuting prostate epithelium when it is cleaved and released from the cell surface by matrilysin (MMP-7) (61). Moreover, Fas/Fas-L proteins are upregulated 1 day after weaning, and Fas/Fas-L–deficient mice have a delay in mammary gland involution (62). We have now initiated studies to address whether members of the TNF-α superfamily are processed differentially to induce altered cell death signaling in *Timp-3*–null mammary tissue.

TIMP-3 and apoptosis. In contrast to our results, several studies have reported that very high expression of TIMP-3 promotes apoptosis (19, 20, 22–25), whereas we demonstrate that TIMP-3 is antiapoptotic in our model. These opposing findings are not surprising given that the systems involved are far from comparable. Some important distinctions are the cell types examined, the quantity of TIMP-3 expressed, and the differences between in vitro cell culture models and in vivo physiological models. For instance, the proapoptotic effect associated with high TIMP-3 has been documented against several cancer cell lines (melanoma, fibrosarcoma, and carcinoma) and smooth muscle cells (19, 21). Our study focused on mammary epithelial cells that are particularly sensitive to

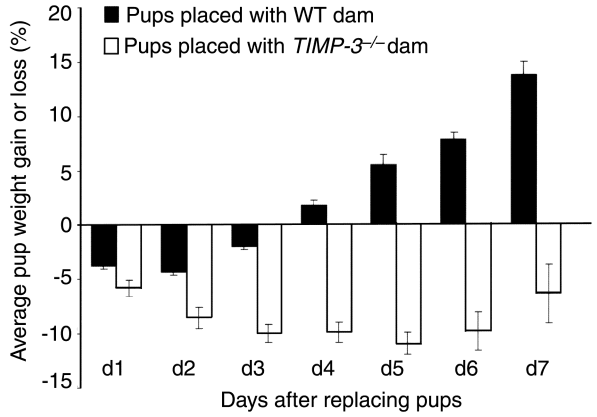

Figure 8
After 2 days of involution, *Timp-3*–null female mice are unable to reinitiate lactation that is necessary for proper pup growth. Quantification of pup weight gain/loss when nursed by wild-type or *Timp-3*–null dams that have already undergone 2 days of involution. Pup weight was measured initially before placing with dams and every subsequent 24 hours. Percent weight gain/loss is calculated by subtracting original weight of pups (12 days of age) from the weight of the same pups at each time point. Weight loss was evident in pups placed with wild-type dams only for the first 3 days, but pup weights accelerated higher thereafter. In contrast, after 7 days, pups placed with *Timp-3*–null female mice failed to gain weight beyond their original weight. Quantification is representative of two separate experiments.

maintaining optimal cell-ECM contact for their survival (63, 64), unlike cancer cells that can enter cell cycle upon detachment from ECM (65). In our model, we provide evidence that ECM degradation is inappropriately prevalent in the absence of TIMP-3. Therefore, mammary epithelial cells within this microenvironment may have compromised cell-ECM adhesion and increased susceptibility toward apoptosis. Second, TIMP-3 is ECM bound, and therefore altered levels of TIMP-3 may mask or expose cellular attachment domains, thereby changing cell-ECM signaling and subsequent survival signals. In fact, TIMP-3 was originally characterized as a factor capable of inducing detachment of cancer cells from their substratum (66). Finally, effects arising from in vitro versus those from in vivo systems are difficult to compare, and even individual physiological systems are likely to respond differentially depending on the makeup of their microenvironment. George et al. (20) induced apoptosis with high levels of adenoviral-delivered TIMP-3 to grafted neointima. We have shown here a proapoptotic effect with *Timp-3* deficiency in regressing mammary gland, but have also found that apoptosis is not a contributing factor during lung alveolar enlargement in *Timp-3*–null mice. Therefore, we propose that the divergent effects of TIMP-3 on cell survival aptly depend on the cell type, the cell microenvironment, and the amount of TIMP-3 in this microenvironment.

Reestablishment of functional lactation is dependent on TIMP-3. In mice, mammary glands are still able to reinitiate lactation after approximately 2 days of involution (34). This ability is, however, lost by 3 days of involution. Here we have demonstrated that *Timp-3*–null female mice are unable to reestablish lactation efficiently and to effectively provide nourishment to pups after 2 days of involution, whereas wild-type mice can. Therefore, TIMP-3 provides the mammary tissue with the ability to maintain and/or reinitiate lactational differentiation after a short period of involution. This is, to our knowledge, the first report to establish that a proteinase inhibitor is essential for one aspect of mammary gland function and further supports the role of proteinases and their inhibitors in controlling multiple aspects of mammary gland involution.

While our current investigations clearly demonstrate that *Timp-3* deficiency within mammary tissue accelerates postlactational epithelial apoptosis, the mechanism(s) underlying these effects remains to be fully elucidated. TIMP-3 has a broad inhibitory capacity toward the MMP and the ADAM family of proteases. Therefore, we envision that multiple molecules impacting specific pathways will converge to enhance cell death and tissue remodeling in *Timp-3*–null tissue. This scenario is especially applicable to the mammary gland given that its form, function, and survival are tightly linked to the extracellular milieu (1). Events amenable to TIMPs modulation include disassembly of cell-cell contacts (67), cell-ECM detachment (68), ligand-receptor interactions (2), and availability of growth factors (13, 48, 69). Distinguishing the causal events from the subsequent consequences is our next challenge.

Acknowledgments

The authors are grateful to O.H. Sanchez, K.L.M. Gowing, C. Hojilla, and M. Johnson for their technical expertise. This work was supported by a Canadian Institutes of Health Research grant to R. Khokha. J.E. Fata was supported by a University of Toronto Open Scholarship; R.A. Moorehead, by a United States Army Medical Research and Materiel Command Postdoctoral Fellowship; and E.B. Voura, by an National Science and Engineering Research Council of Canada Postdoctoral Fellowship.

1. Schmeichel, K.L., Weaver, V.M., and Bissell, M.J. 1998. Structural cues from the tissue microenvironment are essential determinants of the human mammary epithelial cell phenotype. *J. Mammary Gland Biol. Neoplasia.* **3**:201–213.
2. Werb, Z., and Yan, Y. 1998. A cellular striptease act. *Science.* **282**:1279–1280.
3. Blavier, L., Henriet, P., Imren, S., and Declerck, Y.A. 1999. Tissue inhibitors of matrix metalloproteinases in cancer. *Ann. NY Acad. Sci.* **878**:108–119.
4. Gomez, D.E., Alonso, D.F., Yoshiji, H., and Thorgeirsson, U.P. 1997. Tissue inhibitors of metalloproteinases: structure, regulation and biological functions. *Eur. J. Cell Biol.* **74**:111–122.
5. Leco, K.J., Khokha, R., Pavloff, N., Hawkes, S.P, and Edwards, D.R. 1994. Tissue inhibitor of metalloproteinases-3 (TIMP-3) is an extracellular matrix-associated protein with a distinctive pattern of expression in mouse cells and tissues. *J. Biol. Chem.* **269**:9352–9360.
6. Butler, G.S., Apte, S.S., Willenbrock, F., and Murphy, G. 1999. Human tissue inhibitor of metalloproteinases 3 interacts with both the N- and C-terminal domains of gelatinases A and B. Regulation by polyanions. *J. Biol. Chem.* **274**:10846–10851.
7. Yu, W.H., Yu, S., Meng, Q., Brew, K., and Woessner, J.F. 2000. TIMP-3 binds to sulfated glycosaminoglycans of the extracellular matrix. *J. Biol. Chem.* **275**:31226–31232.
8. Weber, B.H., Vogt, G., Pruett, R.C., Stohr, H., and Felbor, U. 1994. Mutations in the tissue inhibitor of metalloproteinases-3 (TIMP3) in patients with Sorsby's fundus dystrophy. *Nat. Genet.* **8**:352–356.
9. Kang, S.H., et al. 2000. Transcriptional inactivation of the tissue inhibitor of metalloproteinase-3 gene by DNA hypermethylation of the 5′-CpG island in human gastric cancer cell lines. *Int. J. Cancer.* **86**:632–635.
10. Pennie, W.D., Hegamyer, G.A., Young, M.R., and Colburn, N.H. 1999. Specific methylation events contribute to the transcriptional repression of the mouse tissue inhibitor of metalloproteinases-3 gene in neoplastic cells. *Cell Growth Differ.* **10**:279–286.
11. Amour, A., et al. 1998. TNF-alpha converting enzyme (TACE) is inhibited by TIMP-3. *FEBS Lett.* **435**:39–44.
12. Lee, M.H., Knauper, V., Becherer, J.D., and Murphy, G. 2001. Full-length and N-TIMP-3 display equal inhibitory activities toward TNF-alpha convertase. *Biochem. Biophys. Res. Commun.* **280**:945–950.
13. Loechel, F., Fox, J.W., Murphy, G., Albrechtsen, R., and Wewer, U.M. 2000. ADAM 12-S cleaves IGFBP-3 and IGFBP-5 and is inhibited by TIMP-3. *Biochem. Biophys. Res. Commun.* **278**:511–515.
14. Kashiwagi, M., Tortorella, M., Nagase, H., and Brew, K. 2001. Timp-3 is a potent inhibitor of aggrecanase 1 (adam-ts4) and aggrecanase 2 (adam-ts5). *J. Biol. Chem.* **276**:12501–12504.
15. Borland, G., Murphy, G., and Ager, A. 1999. Tissue inhibitor of metalloproteinases-3 inhibits shedding of L-selectin from leukocytes. *J. Biol. Chem.* **274**:2810–2815.
16. Fitzgerald, M.L., Wang, Z., Park, P.W., Murphy, G., and Bernfield, M. 2000. Shedding of syndecan-1 and -4 ectodomains is regulated by multiple signaling pathways and mediated by a TIMP-3-sensitive metalloproteinase. *J. Cell Biol.* **148**:811–824.
17. Hargreaves, P.G., et al. 1998. Human myeloma cells shed the interleukin-6 receptor: inhibition by tissue inhibitor of metalloproteinase-3 and a hydroxamate-based metalloproteinase inhibitor. *Br. J. Haematol.* **101**:694–702.
18. Nath, D., Williamson, N.J., Jarvis, R., and Murphy, G. 2001. Shedding of c-Met is regulated by crosstalk between a G-protein coupled receptor and the EGF receptor and is mediated by a TIMP-3 sensitive metalloproteinase. *J. Cell Sci.* **114**:1213–1220.
19. Baker, A.H., Zaltsman, A.B., George, S.J., and Newby, A.C. 1998. Divergent effects of tissue inhibitor of metalloproteinase-1, -2, or -3 overexpression on rat vascular smooth muscle cell invasion, proliferation, and death in vitro. TIMP-3 promotes apoptosis. *J. Clin. Invest.* **101**:1478–1487.
20. George, S.J., Lloyd, C.T., Angelini, G.D., Newby, A.C., and Baker, A.H. 2000. Inhibition of late vein graft neointima formation in human and porcine models by adenovirus-mediated overexpression of tissue inhibitor of metalloproteinase-3. *Circulation.* **101**:296–304.

21. Ahonen, M., Baker, A.H., and Kahari, V.M. 1998. Adenovirus-mediated gene delivery of tissue inhibitor of metalloproteinases-3 inhibits invasion and induces apoptosis in melanoma cells. *Cancer Res.* **58**:2310–2315.
22. Baker, A.H., George, S.J., Zaltsman, A.B., Murphy, G., and Newby, A.C. 1999. Inhibition of invasion and induction of apoptotic cell death of cancer cell lines by overexpression of TIMP-3. *Br. J. Cancer.* **79**:1347–1355.
23. Smith, M.R., Kung, H., Durum, S.K., Colburn, N.H., and Sun., Y. 1997. TIMP-3 induces cell death by stabilizing TNF-alpha receptors on the surface of human colon carcinoma cells. *Cytokine.* **9**:770–780.
24. Bian, J., et al. 1996. Suppression of in vivo tumor growth and induction of suspension cell death by tissue inhibitor of metalloproteinases (TIMP)-3. *Carcinogenesis.* **17**:1805–1811.
25. Bond, M., et al. 2000. Localization of the death domain of tissue inhibitor of metalloproteinase-3 to the N terminus. Metalloproteinase inhibition is associated with proapoptotic activity. *J. Biol. Chem.* **275**:41358–41363.
26. Leco, K.J., et al. 2001. Spontaneous air space enlargement in the lungs of mice lacking tissue inhibitor of metalloproteinases-3 (TIMP-3). *J. Clin. Invest.* **108**:817–829.
27. Fata, J.E., Ho, A., Leco, K.J., Moorehead, R.A., and Khokha, R. 2000. Cellular turnover and extracellular matrix remodeling in female reproductive tissues: functions of metalloproteinases and their inhibitors. *Cell. Moll. Life Sciences.* **57**:77–95.
28. Mayhew, T.M., Myklebust, R., Whybrow, A., and Jenkins, R. 1999. Epithelial integrity, cell death and cell loss in mammalian small intestine. *Histol. Histopathol.* **14**:257–267.
29. Reynaud, K., and Driancourt, M.A. 2000. Oocyte attrition. *Mol. Cell Endocrinol.* **163**:101–108.
30. Sorisky, A., Magun, R., and Gagnon, A.M. 2000. Adipose cell apoptosis: death in the energy depot. *Int. J. Obes. Relat. Metab. Disord.* **4**(Suppl.):S1–S7.
31. Wilde, C.J., Knight, C.H., and Flint, D.J. 1999. Control of milk secretion and apoptosis during mammary involution. *J. Mammary Gland Biol. Neoplasia.* **4**:129–136.
32. Quarrie, L.H., Addey, C.V., and Wilde, C.J. 1996. Programmed cell death during mammary tissue involution induced by weaning, litter removal, and milk stasis. *J. Cell Physiol.* **168**:559–569.
33. Marti, A., Feng, Z., Altermatt, H.J., and Jaggi, R. 1997. Milk accumulation triggers apoptosis of mammary epithelial cells. *Eur. J. Cell Biol.* **73**:158–165.
34. Lund, L.R., et al. 1996. Two distinct phases of apoptosis in mammary gland involution: proteinase-independent and -dependent pathways. *Development.* **122**:181–193.
35. Li, M., et al. 1997. Mammary-derived signals activate programmed cell death during the first stage of mammary gland involution. *Proc. Natl. Acad. Sci. USA.* **94**:3425–3430.
36. Alexander, C.M., Selvarajan, S., Mudgett, J., and Werb, Z. 2001. Stromelysin-1 regulates adipogenesis during mammary gland involution. *J. Cell Biol.* **152**:693–703.
37. Uria, J.A., and Werb, Z. 1998. Matrix metalloproteinases and their expression in mammary gland. *Cell. Res.* **8**:187–194.
38. Ossowski, L., Biegel, D., and Reich, E. 1979. Mammary plasminogen activator: correlation with involution, hormonal modulation and comparison between normal and neoplastic tissue. *Cell.* **16**:929–940.
39. Dickson, S.R., and Warburton, M.J. 1992. Enhanced synthesis of gelatinase and stromelysin by myoepithelial cells during involution of the rat mammary gland. *J. Histochem. Cytochem.* **40**:697–703.
40. Lefebvre, O., et al. 1992. The breast cancer-associated stromelysin-3 gene is expressed during mouse mammary gland apoptosis. *J. Cell Biol.* **119**:997–1002.
41. Talhouk, R.S., Bissell, M.J., and Werb, Z. 1992. Coordinated expression of extracellular matrix-degrading proteinases and their inhibitors regulates mammary epithelial function during involution. *J. Cell Biol.* **118**:1271–1282.
42. Talhouk, R.S., Chin, J.R., Unemori, E.N., Werb, Z., and Bissell, M.J. 1991. Proteinases of the mammary gland: developmental regulation in vivo and vectorial secretion in culture. *Development.* **112**:439–449.
43. Strange, R., Li, F., Saurer, S., Burkhardt, A., and Friis, R.R. 1992. Apoptotic cell death and tissue remodeling during mouse mammary gland involution. *Development.* **115**:49–58.
44. Fata, J.E., Leco, K.J., Moorehead, R.A., Martin, D.C., and Khokha, R. 1999. Timp-1 is important for epithelial proliferation and branching morphogenesis during mouse mammary development. *Dev. Biol.* **211**:238–254.
45. Fata, J.E., et al. 2000. The osteoclast differentiation factor osteoprotegerin-ligand is essential for mammary gland development. *Cell.* **103**:41–50.
46. Kimata, K., Sakakura, T., Inaguma, Y., Kato, M., and Nishizuka, Y. 1985. Participation of two different mesenchymes in the developing mouse mammary gland: synthesis of basement membrane components by fat pad precursor cells. *J. Embryol. Exp. Morphol.* **89**:243–257.
47. Schedin, P., Strange, R., Mitrenga, T., Wolfe, P., and Kaeck, M. 2000. Fibronectin fragments induce MMP activity in mouse mammary epithelial cells: evidence for a role in mammary tissue remodeling. *J. Cell Sci.* **113**:795–806.
48. Fata, J.E., Chaudhary, V., and Khokha, R. 2001. Cellular turnover in the mammary gland is correlated with the systemic levels of progesterone and not 17-beta-estradiol during the estrous cycle. *Biol. Reprod.* **65**:680–688.
49. Will, H., Atkinson, S.J., Butler, G.S., Smith, B., and Murphy, G. 1996. The soluble catalytic domain of membrane type 1 matrix metalloproteinase cleaves the propeptide of progelatinase A and initiates autoproteolytic activation. Regulation by TIMP-2 and TIMP-3. *J. Biol. Chem.* **271**:17119–17123.
50. Sato, H., et al. 1996. Cell surface binding and activation of gelatinase A induced by expression of membrane-type-1-matrix metalloproteinase (MT1-MMP). *FEBS Lett.* **385**:238–240.
51. Werb, Z., Tremble, P.M., Behrendtsen, O., Crowley, E., and Damsky C.H. 1989. Signal transduction through the fibronectin receptor induces collagenase and stromelysin gene expression. *J. Cell Biol.* **109**:877–889.
52. Stanton, H., et al. 1998. The activation of ProMMP-2 (gelatinase A) by HT1080 fibrosarcoma cells is promoted by culture on a fibronectin substrate and is concomitant with an increase in processing of MT1-MMP (MMP-14) to a 45 kDa form. *J. Cell Sci.* **111**:2789–2798.
53. Monaghan, P., Warburton, M.J., Perusinghe, N., and Rudland, P.S. 1983. Topographical arrangement of basement membrane proteins in lactating rat mammary gland: comparison of the distribution of type IV collagen, laminin, fibronectin, and Thy-1 at the ultrastructural level. *Proc. Natl. Acad. Sci. USA.* **80**:3344–3348.
54. Almeida, E.A., et al. 2000. Matrix survival signaling: from fibronectin via focal adhesion kinase to c-Jun NH(2)-terminal kinase. *J. Cell Biol.* **149**:741–754.
55. Ilic, D., et al. 1998. Extracellular matrix survival signals transduced by focal adhesion kinase suppress p53-mediated apoptosis. *J. Cell Biol.* **143**:547–560.
56. Kapila, Y.L., Wang, S., and Johnson, P.W. 1999. Mutations in the heparin binding domain of fibronectin in cooperation with the V region induce decreases in pp125(FAK) levels plus proteoglycan-mediated apoptosis via caspases. *J. Biol. Chem.* **274**:30906–30913.
57. Dickson, S.R., and Warburton M.J. 1992. Enhanced synthesis of gelatinase and stromelysin by myoepithelial cells during involution of the rat mammary gland. *J. Histochem. Cytochem.* **40**:697–703.
58. Killar, L., White, J., Black, R., and Peschon, J. 1999. Adamalysins. A family of metzincins including TNF-alpha converting enzyme (TACE). *Ann. NY Acad. Sci.* **878**:442–452.
59. Varela, L.M., and Ip, M.M. 1996. Tumor necrosis factor-alpha: a multifunctional regulator of mammary gland development. *Endocrinology.* **137**:4915–4924.
60. Rewinski, M.J., and Yang, T.J. 1994. Lactation stage-dependent changes in levels of tumor necrosis factor/cachectin in milk. *Am. J. Reprod. Immunol.* **31**:170–176.
61. Powell, W.C., Fingleton, B., Wilson, C.L., Boothby, M., and Matrisian, L.M. 1999. The metalloproteinase matrilysin proteolytically generates active soluble Fas ligand and potentiates epithelial cell apoptosis. *Curr. Biol.* **9**:1441–1447.
62. Song, J., et al. 2000. Roles of Fas and Fas ligand during mammary gland remodeling. *J. Clin. Invest.* **106**:1209–1220.
63. Boudreau, N., Sympson, C.J., Werb, Z., and Bissell, M.J. 1995. Suppression of ICE and apoptosis in mammary epithelial cells by extracellular matrix. *Science.* **267**:891–893.
64. Boudreau, N., Werb, Z., and Bissell., M.J. 1996. Suppression of apoptosis by basement membrane requires three-dimensional tissue organization and withdrawal from the cell cycle. *Proc. Natl. Acad. Sci. USA.* **93**:3509–3513.
65. Reed, J.C. 1999. Dysregulation of apoptosis in cancer. *J. Clin. Oncol.* **17**:2941–2953.
66. Blenis, J., and Hawkes, S.P. 1983. Transformation-sensitive protein associated with the cell substratum of chicken embryo fibroblasts. *Proc. Natl. Acad. Sci. USA.* **80**:770–774.
67. Noe, V., et al. 2001. Release of an invasion promoter E-cadherin fragment by matrilysin and stromelysin-1. *J. Cell Sci.* **114**:111–118.
68. Merio, G.R., Cella, N., and Hynes, N.E. 1997. Apoptosis is accompanied by changes in Bcl-2 and Bax expression, induced by loss of attachment, and inhibited by specific extracellular matrix proteins in mammary epithelial cells. *Cell Growth Differ.* **8**:251–260.
69. Martin, D.C., Fowlkes, J.L., Babic, B., and Khokha, R. 1999. Insulin-like growth factor II signaling in neoplastic proliferation is blocked by transgenic expression of the metalloproteinase inhibitor TIMP-1. *J. Cell Biol.* **146**:881–892.